AD-A084 233 TEXAS UNIV AT AUSTIN DEPT OF COMPUTER SCIENCES F/G 9/4
EDGE DETECTION IN TEXTURES.(U)
OCT 79 L S DAVIS, A MITICHE F49620-79-C-0043
UNCLASSIFIED TR-111 AFOSR -TR-80-0415 NL

1 OF 1
AD
A084233

END
DATE
FILMED
6 80
DTIC

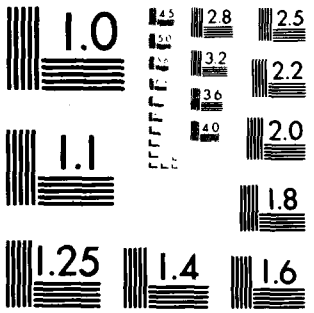


MICROCOPY RESOLUTION TEST CHART
NATIONAL BUREAU OF STANDARDS 1963 A

AFOSR-TR- 80-0415

ADA084233

# EDGE DETECTION IN TEXTURES

Larry S. Davis
Amar Mitiche

Computer Sciences Department
The University of Texas at Austin
Austin, Texas 78712

TR-111 October 1979

DTIC
ELECTE
MAY 16 1980
A

DDC FILE COPY

411753

This research was supported in part by funds derived from the Air Force Office of Scientific Research under contract F49620-79-C-0043

80 5 14 077

Approved for public release; distribution unlimited.

UNCLASSIFIED

SECURITY CLASSIFICATION OF THIS PAGE (When Data Entered)

# REPORT DOCUMENTATION PAGE

READ INSTRUCTIONS BEFORE COMPLETING FORM

1. REPORT NUMBER: 18 AFOSR-TR-80-0415
2. GOVT ACCESSION NO. AD-A084233
3. RECIPIENT'S CATALOG NUMBER

4. TITLE (and Subtitle): 6 EDGE DETECTION IN TEXTURES.

5. TYPE OF REPORT & PERIOD COVERED: 9 Interim rept.

6. PERFORMING ORG. REPORT NUMBER

7. AUTHOR(s): 10 Larry S. Davis, Amar Mitiche

8. CONTRACT OR GRANT NUMBER(s): 15 F49620-79-C-0043

9. PERFORMING ORGANIZATION NAME AND ADDRESS:
University of Texas at Austin
Department of Computer Sciences
Austin, TX 78712
17 A2

10. PROGRAM ELEMENT, PROJECT, TASK AREA & WORK UNIT NUMBERS: 16 61102F 2304/A2

11. CONTROLLING OFFICE NAME AND ADDRESS:
Air Force Office of Scientific Research/NM
Bolling AFB, Washington, DC 20332
11

12. REPORT DATE: Oct[redacted]79

13. NUMBER OF PAGES: 29

14. MONITORING AGENCY NAME & ADDRESS (if different from Controlling Office): 12 30

15. SECURITY CLASS. (of this report): UNCLASSIFIED

15a. DECLASSIFICATION/DOWNGRADING SCHEDULE

16. DISTRIBUTION STATEMENT (of this Report)
Approved for public release; distribution unlimited.

14 TR-111

17. DISTRIBUTION STATEMENT (of the abstract entered in Block 20, if different from Report)

DTIC ELECTE MAY 16 1980 A

18. SUPPLEMENTARY NOTES

19. KEY WORDS (Continue on reverse side if necessary and identify by block number)
image processing, texture, edge detection

411753

20. ABSTRACT (Continue on reverse side if necessary and identify by block number)

Detecting edges is an important first step in the solution of many image analysis tasks. Edges are usedprimarily to aid in the segmentation of an image into meaningful regions, but are also extensively used to computer relatively local measures of textural variation (whic, of course, can subsequently be used for segmentation purposes). Although there has been a considerable amount of research concerning quantitative models for edge detection, very little work has been devoted to developing such models for images described by texture models.

DD FORM 1 JAN 73 1473 EDITION OF 1 NOV 65 IS OBSOLETE

UNCLASSIFIED

## 1. Introduction

Detecting edges is an important first step in the solution of many image analysis tasks. Edges are used primarily to aid in the segmentation of an image into meaningful regions, but are also extensively used to compute relatively local measures of textural variation (which, of course, can subsequently be used for segmentation purposes). Although there has been a considerable amount of research concerning quantitative models for edge detection (e.g., Nahi [1], Modestino and Fries [2], Shanmugan et al [3], Cooper and Elliot [4]), very little work has been devoted to developing such models for images described by texture models. This paper addresses the problem of detecting edges in what are called macro-textures, i.e., cellular textures where the cells, or texture elements, are relatively large (at least several pixels in diameter).

Once edges are detected in texture regions, they can be used to define texture descriptors in a variety of ways. For example, one can compute "edge per unit area" (Rosenfeld [5]). More generally, one can compute first-order statistics of edge properties [6,7], such as orientation, contrast, fuzziness, etc., or higher-order statistics which can measure the spatial arrangement of edges in the texture. Such statistics can be computed from generalized cooccurrence matrices (Davis et al [8,9]) which count the number of times that specific pairs of edges occur in specific relative spatial positions. Clearly, the utility of such tools depends on the reliability with which edges can be detected in textures.

This paper is organized as follows: Section 2 contains a description

of the image texture models which will be considered. These models are one-dimensional, since the edge-detection procedures, described in Section 3, are one-dimensional. Section 4 contains derivations of the expected value and variance of the edge operator described in Section 3 and describes optimal edge detection procedures based on that analysis. Finally, Section 5 contains conclusions and a summary.

AIR F[illegible] SCIENTIFIC RESEARCH (AFSC)
NOTICE [illegible]
Th[illegible] and is
a[illegible] 190-12 (7b).
Di[illegible].
A. D. B[illegible]
Technical Information Officer

## 2. Texture Models

There are a large number of formal image texture models which have been proposed and studied during the past few years. These can be broadly classified as pixel-based and region-based models (Ahuja [10]). All of these models treat textures as a two-dimensional phenomena, which is appropriate for many applications (e.g., some medical applications, geographical applications). However, for other applications, regarding textures in this way is inappropriate; one should, instead, model the texture as a surface in space with certain reflectance properties. An image of such a texture is then determined by the spatial disposition of the surface and the viewer, the frequency response of the viewer, and the positions of all light sources. Horn [11] should be consulted for an introduction to this branch of image science. Such models will not be considered in this paper.

Pixel-based models are ordinarily time-series models or random field models. Time-series models have been investigated by McCormick and Jayaramamurthy [12], and by Tou et al [13]. Random field models are discussed in Wong [14], and Pratt et al [15]. For more references, see [16-17].

This paper will be concerned with region-based texture models. In particular, we will consider one-dimensional models which are related to two-dimensional cell structure models. Cell structure models describe textures as mosaics, and can be generated by the following two-step process:

1) A planar region is tessellated into cells, ordinarily convex.

2) Each cell is independently assigned one of m colors, $c_1,\ldots,c_m$, using a fixed set of probabilities, $p_1,\ldots,p_m$.

This process partitions the original region into subregions, which are the unions of cells of constant color. If A is the original region, then $A_1,\ldots,A_m$ are the subregions. Note that the simple colors can be replaced by more complex coloring processes, e.g., the grey levels in a cell can be chosen according to a given distribution, d, which is itself chosen from a set of distributions, D, according to the given probability vector, P. Ahuja [10] contains an extensive survey of such models.

We will consider a similar class of one-dimensional models. A texture model is an ordered pair <P,C> where

1) P is a cell width model, which successively drops intervals along a line, and

2) C is a coloring model, consisting of coloring processes, $c_1,\ldots,c_m$, and probabilities, $p_1,\ldots,p_m$. As P produces cells, C colors the cells.

If we let w be the random variable corresponding to cell width, then the following are examples of cell width models:

1) Constant cell width model

$$P_c(w) = \begin{cases} 1 & w=b \\ 0 & w\neq b \end{cases}$$

2) Uniform cell width model

$$P_u(w) = \begin{cases} 1/b & 0 \leq w \leq b \\ 0 & w > b \end{cases}$$

3) Exponential cell width model

$$P_e(w) = \lambda \exp[\lambda w].$$

To simplify the analysis, we assume that there are only two coloring processes, $c_1$ and $c_2$. Therefore, there is only one relevant probability for choosing cell colors, which will be denoted by p. Each coloring process colors a cell by choosing the intensity of each point in that cell independently from a normal distribution of intensities. The distributions are denoted $N(m_i, v_i)$, $i=1,2$, with mean $m_i$ and variance $v_i$.

Notice that given a one-dimensional cell structure model, $\langle P,C \rangle$, one can derive a one-dimensional <u>component</u> structure model, where a component is a contiguous set of identically colored cells. For example, for the cell model $\langle P_c,C \rangle$ the corresponding component model has components whose lengths are distributed geometrically. Of course, in a component model, the various colors alternate, since by definition two adjacent components must have different colors. The component model is required to determine the prior probabilities of various types of pixels (see Section 4).

## 3. A One-Dimensional Edge-Detector

In this section we will describe a simple, one-dimensional edge detection procedure. There are a variety of reasons for considering one-dimensional edge detectors:

1) Computational efficiency on conventional, sequential computers. Since we are interested in detecting edges for the purpose of describing texture, it is important that the edge detection process be made as efficient as possible.

2) Suitability for implementation on special-purpose image processing hardware. There has been a significant amount of research and development of image processing hardware over the past few years (CLIP [18], PICAP [19]). One-dimensional edge detectors can be easily implemented on, for example, series-parallel machines, where a row of processors "scan" and process the image one row at a time.

3) Mathematical tractability. Direct analysis of two-dimensional edge detectors is complicated by many factors, including the mathematical complexity of most two-dimensional cellular texture models and the greater variety of edge-like features in two dimensions.

The class of edge operators which we have considered is based on differences of averages between adjacent, symmetric one-dimensional image neighborhoods. Specifically, let f be a one-dimensional image function. Then the edge operator is:

$$e_k(i) = (1/k) \sum_{j=1}^{k} (f(i-j)-f(i+j))$$

$$= (1/k)\ (LS(i)-RS(i))$$

where

$$LS(i) = \sum_{j=1}^{k} f(i-j) \quad \text{and}$$

$$RS(i) = \sum_{j=1}^{k} f(i+j)$$

By noticing that

$$e_k(i+1) = (1/k)\ [LS(i)-f(i-k) + f(i)-RS(i) + f(i+1)-f(i+k+1)]$$

we see that $e_k$ can be computed in a constant number of operations per picture point, independent of k, on a conventional sequential computer.

The operator $e_k$ is used to detect edges by the following three step process:

1) Compute $e_k(i)$ for all points i.

2) Discard all i with $|e_k(i)| < t$. This <u>thresholding</u> step is intended to discriminate between points which are edges of texture elements and points which are in the interior of texture elements, but far from edges.

3) Discard all i with $|e_k(i)| < |e_k(i+j)|$, $|j| < d$. This <u>non-maxima suppression</u> step is intended to discriminate between points which are edges and points which are interior to texture elements, but are close to edges.

Step 3 is crucial since $e_k$ gives high response not just at edges, but also near edges, so that thresholding alone would result in a cluster of detections about each true edge point. The above procedure involves three classes of texture pixels:

1) <u>edge pixels</u>, which are pixels located directly at the edges between texture elements;

2) <u>near-edge pixels</u>, which are located within distance d of an

edge pixel and are discarded by the non-maxima suppression step; and

3) interior pixels, which are located distances greater than d from the nearest edge pixel, and are ordinarily eliminated by the thresholding step (but may be eliminated due to proximity to above threshold, near-edge pixels).

Optimizing the above edge detection procedure involves choosing k, t and d in order to minimize the probability of error--i.e., minimizing the frequency of discarding edge points, and not discarding near-edge and interior pixels. This paper considers the edge-interior discrimination problem only. Therefore, we will be concerned with choosing values for k and t only. The complete edge detector, including the non-maxima suppression step, is discussed in Davis and Mitiche [20].

## 4. Analysis of $e_k$

In this section we will derive the expected value and variance of $e_k$ at edges and at interior points. We will regard an interior point as a point whose distance from the nearest edge is greater than k. Expressions for the prior probabilities of edge and interior points are developed. Finally, by assuming that $e_k$ is normally distributed at edges and interiors, a minimum error thresholding procedure for distinguishing between edge points and interior points is developed.

### 4.1 The expected value of $e_k$, $E[e_k]$

The definition of $e_k$ was originally given for a discrete function f. If f is continuous, then we can redefine $e_k$ as

$$e_k(i) = 1/k \left[ \int_{-k}^{0} f(i+j)dj - \int_{0}^{k} f(i+j)dj \right]$$

Then, the expected value of $e_k$ is

$$E[e_k(i)] = 1/k \left[ \int_{-k}^{0} E[f(i+j)]dj - \int_{0}^{k} E[f(i+j)]dj \right]$$

If i is an interior point, then all points $f(i+j)$, $-k \leq j \leq k$ are colored by the same process. Therefore, the expected values are all the same, and thus $E[e_k(i) | i \text{ is an interior point}] = 0$.

Now suppose that i is an edge point, and assume, without loss of generality, that the cell to the left of i, $C_\ell$, is colored by process $c_1$, and that the cell to the right of i, $C_r$, is colored by by process $c_2$, and that $m_1 > m_2$. Let $w_\ell$ be the width of $C_\ell$ and $w_r$ be the width of $C_r$ (see Figure 1). We will also make the simplifying assumption that the points

to the left of $C_\ell$ (or the right of $C_r$) are individually colored with processes $c_1$ and $c_2$ with probabilities p and (1-p). For k much greater than $w_\ell$ or $w_r$, this assumption is not unreasonable. As $w_\ell$ or $w_r$ approaches k, it is more likely that only one cell will be found to the left of $C_\ell$ or the right of $C_r$. However, large cells are ordinarily less likely than small cells. Letting $a = pm_1 + (1-p)m_2$, we can then write

$$E[e_k(i)] = 1/k \left[ \left( \int_0^k (m_1 w_\ell + a(k-w_\ell)P(w_\ell)dw_\ell + \int_k^\infty m_1 kP(w_\ell)dw_\ell \right) \right.$$

$$\left. - \int_0^k (m_2 w_r + a(k-w_r)P(w_r)dw_r + \int_k^\infty m_2 kP(w_r)dw_r) \right]$$

Since $w_\ell$ and $w_r$ are drawn from the same distribution, terms can be grouped to obtain

$$E[e_k(i)] = 1/k \left[ \int_0^k (m_1-m_2)wP(w)dw + \int_k^\infty (m_1-m_2)kP(w)dw \right]$$

$$= 1/k \left[ (m_1-m_2)w_0 - \int_k^\infty (m_1-m_2)wP(w)dw + \int_k^\infty (m_1-m_2)kP(w)dw \right]$$

$$= \frac{(m_1-m_2)}{k} \left[ w_0 - \int_k^\infty (w-k)P(w)dw \right]$$

where

$$w_0 = \int_0^\infty wP(w)dw.$$

4.2 The variance of $e_k$

From the definition of $e_k$, we have

$$\text{Var}\ [e_k(i)] = \text{Var} \left[ 1/k \int_0^k f(i-j)-f(i+j)dj \right]$$

Suppose i is an interior point and is in a cell colored by $c_1$. Then

$$\mathrm{Var}[e_k(i)] = (1/k^2)\, k\, 2v_1$$

$$= 2v_1/k$$

If i is an interior point and is in a cell colored by $c_2$, then $\mathrm{Var}[e_k(i)] = 2v_2/k$.

Next we will consider the case of i, an edge point. Let

$$LS(i) = \int_0^k f(i-j)dj$$

$$RS(i) = \int_0^k f(i+j)dj$$

Then

$$e_k(i) = 1/k\ (LS(i)-RS(i))$$

We will derive expressions for Var[LS(i)] and Var[RS(i)]. There are two cases to consider:

1) $w_\ell$ or $w_r \geq k$
2) $w_\ell$ or $w_r < k$

If $w_\ell \geq k$, then the variance of LS(i) is $kv_1$. If $w_r \geq k$, then the variance of RS(i) is $kv_2$.

Next, suppose $w_\ell < k$. We will assume that of the $k-w_\ell$ pixels not in $C_\ell$, $\ell_1$ pixels are colored by process $c_1$ and $\ell_2 = (k-w_\ell)-\ell_1$ pixels are colored by process $c_2$, where $\ell_1$ is a random variable described by a binomial distribution with parameter p and $\ell_2$ is a random variable described by a binomial distribution with parameter (1-p).

In general, if y is the sum of a random number, n, of independent

experimental values of a random variable x, then

$$\mathrm{Var}[y] = E[n]\ \mathrm{Var}[x] + (E[x])^2\ \mathrm{Var}[n]$$

Thus, if $w_\ell$ is a fixed value less than k,

$$\mathrm{Var}[LS(i)|w_\ell < k] =$$

$$w_\ell v_1 + E[\ell_1]v_1 + m_1^2\ \mathrm{Var}[\ell_1]$$
$$+ E[\ell_2]v_2 + m_2^2\ \mathrm{Var}[\ell_2]$$

with

$$E[\ell_1] = (k-w_\ell)p$$

$$E[\ell_2] = (k-w_\ell)(1-p)$$

$$\mathrm{Var}[\ell_1] = \mathrm{Var}[\ell_2] = (k-w_\ell)\ p(1-p)$$

A similar expression can be obtained for RS(i).

Combining the cases $w_\ell \geq k$ and $w_\ell < k$, we can write

$$\mathrm{Var}[LS(i)|i \text{ an edge}] =$$

$$\frac{1}{k^2}\Big[\int_k^\infty kv_1 P(w_\ell)dw_\ell$$
$$+ \int_0^k (w_\ell v_1 + (k-w_\ell)(pv_1 + (1-p)v_2)$$
$$+ (k-w_\ell)\ p(1-p)(m_1^2 + m_2^2))\ P(w_\ell)dw_\ell\Big]$$

Again, a similar expression is obtained for RS(i). Since

$$\mathrm{Var}[e_k(i)] = 1/k^2\ [\mathrm{Var}[LS(i)] + \mathrm{Var}[RS(i)]]$$

Since $w_\ell$ and $w_r$ are drawn from the same distribution, we group terms and

$p_e$, and of an interior point, $p_i$. An edge point is defined to be a point on the image line which is no more than a fixed distance d away from a true edge. We choose $d > 0$ so that $p_i \neq 0$. An interior point, as before, is a point that is at least distance k away from a true edge.

In the following we will consider, without loss of generality, only points within $c_1$-components. Given that a point is picked at random, let h be the probability density function for the distance $y_1$ to the next edge (the forward edge or edge on the right). From general results on random incidence into a renewal process we have [21]

$$h(y_1) = (1-\text{prob}[r \leq y_1])/E[r]$$

The function h is also the probability density function for the distance $y_2$ to the backward edge (the nearest edge on the left of the point). Then we have

$$h_j(y_1,y_2) = h(y_1)h_c(y_2/y_1)$$

where $h_c$ is the conditional probability function for $y_2$ and $h_j$ is the joint probability function for $y_1$ and $y_2$. If $y_1$ and $y_2$ are independent, then

$$h_j(y_1,y_2) = h(y_1)h(y_2)$$

From the above we now can derive expressions for the priors

$$p_i = \int_k^\infty \int_k^\infty h_j(y_1,y_2)dy_1dy_2$$

$$p_e = 1 - \int_d^\infty \int_d^\infty h_j(y_1,y_2)dy_1dy_2$$

For the discrete case we have

$$p_i = \sum_{y_1=k}^{\infty} \sum_{y_2=k}^{\infty} h(y_1,y_2)$$

$$p_e = 1 - \sum_{y_1=d+1} \sum_{y_2=d+1} h(y_1,y_2)$$

The set of interior points and the set of edge points are not complementary in the sense that they do not form a partition of the set of all points of the image line. Thus it is necessary that we normalize $p_e$ and $p_i$.

$$p_e \leftarrow p_e/(p_e + p_i)$$

$$p_i \leftarrow p_i/(p_e + p_i)$$

Examples

1. Geometric distribution of component widths. Assume for simplicity that $b = 1$. Then

$$h(y_1) = (1-p)(1 - \sum_{y=1}^{y_1} (1-p)p^{y-1})$$

$$= (1-p) \sum_{y>y_1} (1-p)p^{y-1}$$

$$= (1-p)p^{y_1}$$

Thus

$$\text{Prob}[y_1 \geq k] = \sum_{y_1=k}^{\infty} (1-p)p^{y_1}$$

$$= p \sum_{y_1=k}^{\infty} (1-p)p^{y_1-1}$$

$$= p\,p^{k-1} = p^k$$

$$E[r] = E[n]\,E[w]$$

$$Var[r] = E[n]\,Var[w] + (E[w])^2\,Var[n]$$

If w is continuous and if f and g are the probability density functions for w and r, then

$$g^T(s) = p_\ell^T(f^T(s))$$

where $f^T$ and $g^T$ are the exponential transforms (s-transforms) of f and g respectively, and $p_\ell^T$ is the z-transform (discrete transform) of $p_\ell$.

If w is discrete, then the above expression holds with f and g being the probability mass functions for w and r, and $f^T$ and $g^T$ being their respective z-transforms. By taking the inverse transforms one can obtain the distribution of component widths.

Examples

1. Constant distribution of cell width. For the constant cell width model, g is described by the geometric probability mass function

$$g(r) = \begin{cases} (1-p)\,p^{\frac{r}{b}-1} & \text{for } r = b, 2b, 3b, \ldots \\ 0 & \text{otherwise} \end{cases}$$

$$E[r] = b/(1-p)$$

$$Var[r] = b^2\,p/(1-p)^2$$

2. Exponential distribution of cell width. For the exponential model with parameter $\lambda$, g is described by the probability density function

$$g(r) = (1-p)\,\lambda\,\mathrm{Exp}(-(1-p)\,\lambda r)$$

Thus component widths are still exponentially distributed and

$$E[r] = 1/((1-p)\lambda)$$

3. Uniform distribution of cell width.

$$E[r] = b/(2(1-p))$$

$$\mathrm{Var}[r] = \frac{b/(4(1-p))}{(1/3 + p/(1-p))}$$

and

$$g(r) = e^{(p/b)r}\, g'(r)$$

where

$$g'(r) = (1-p)\left[\sum_{n=0}^{\infty} \frac{(-1)^n p^n e^{-np}}{b^{n+1}} \frac{(r-bn)^n}{\Gamma(n+1)} S_{bn}(r) - \frac{1}{e^p} \sum_{n=0}^{\infty} \frac{(-1)^n p^n e^{-np}}{b^{n+1}} \frac{[r-b(n+1)]^n}{\Gamma(n+1)} S_{b(n+1)}(r)\right]$$

and

$$S_k(t) = \begin{cases} 0 & 0 < t < k \\ 1 & t \geq k \end{cases}$$

is the unit step function.

In order to perform minimum error thresholding on a given image texture, it is necessary to know the prior probabilities of an edge point,

finally obtain, for edge points,

$$\mathrm{Var}[e_k(i)|i \text{ is an edge}] =$$

$$1/k^2 \Big[ k(v_1+v_2) \int_k^\infty P(w)dw$$

$$+ (v_1+v_2) \int_0^k wP(w)dw$$

$$+ 2(pv_1+(1-p)v_2) \int_0^k (k-w)P(w)dw$$

$$+ 2p(1-p)(m_1^2+m_2^2) \int_0^k (k-w)P(w)dw \Big]$$

For the exponential model with $p = .5$, for example, we find that

$$E[e_k(i)|i \text{ is an edge}] = \frac{(m_1-m_2)(1-e^{-\lambda k})}{\lambda k}$$

and

$$\mathrm{Var}[e_k(i)|i \text{ is an edge}] = \frac{(v_1+v_2)}{k} + \frac{m_1^2+m_2^2}{2k}\left(1 - \frac{1-e^{-\lambda k}}{\lambda k}\right)$$

Other simple expressions can be obtained for the constant and uniform models.

In order to derive a minimum error threshold for discriminating between edge and interior points using $e_k$, it is necessary to:

1) determine the prior probabilities of edge and interior points, and

2) specify a form for the distribution of $e_k$ at edges and at interior points.

To compute the prior probabilities of edge and interior point, we must derive a <u>component model</u> from the cell width model. A component is a set of connected, identically colored cells. Let a $c_1$-component ($c_2$-component) be a component whose cells are colored by process $c_1$ ($c_2$). Then, the length of a component is defined to be the number of cells that compose it, and the width of a component is its actual measure.

In the following we will show how a component model can be derived from a cell model. As mentioned before, the cell coloring process is a Bernoulli process which selects coloring process $c_1$ with probability p and coloring process $c_2$ with probability (1-p). Therefore, the $c_1$-component and $c_2$-component lengths are random variables described by a geometric probability mass function. In the following analysis we will consider only $c_1$-components and simply refer to them as components. The same analysis will hold for $c_2$-components.

If n is the random variable that represents component length and $p_\ell(n)$ is the probability mass function for it, then

$$p_\ell(n) = (1-p)\, p^{n-1}$$

Now, if w and r are random variables that describe the cell width and the component width respectively, then r is the sum of a random number n of independent identically distributed experimental values of x:

$$r = \sum_{i=1}^{n} x_i$$

Expressions for the expected value and variance of r can be obtained in terms of the expected value and variance of n and w:

Since the geometric distribution is memoryless, $y_1$ and $y_2$ are independent random variables, and

$$p_i = \text{Prob}[y_1 \geq k,\ y_2 \geq k] = p^k p^k = p^{2k}$$

$$p_e = 1 - p^{2(d+1)}$$

Normalizing,

$$p_i = p^{2k}/(p^{2k} + 1 - p^{2(d+1)})$$

$$p_e = 1 - p_i$$

2. Exponential distribution of component widths. Let $\lambda$ be the parameter of the distribution. Then

$$h(y_1) = \frac{1 - (1 - \text{Exp}(-\lambda y_1))}{1/\lambda} = \lambda\ \text{Exp}(-\lambda y_1)$$

$$\text{Prob}[y_1 \geq k] = \text{Exp}(-\lambda k)$$

The exponential distribution is also memoryless so that $y_1$ and $y_2$ are independent. We then have

$$p_i = \text{Exp}(-2\lambda k)$$

$$p_e = 1 - \text{Exp}(-2d\lambda)$$

Normalizing,

$$p_i = \text{Exp}(-2\lambda k)/(\text{Exp}(-2\lambda k) + 1 - \text{Exp}(-2d\lambda))$$

$$p_e = 1 - p_i$$

In order to use $p_e$, $p_i$ and the expected values obtained above for minimum error edge detection, we will make the assumption that $e_k$ is normally distributed at edge points as well as interior points. More precisely, we assume that $e_k$ is $N(0,2v/k)$ at interior points and $N(E[e_k],Var[e_k])$ at edges. This assumption is certainly valid for interior points since, in this case, LS and RS are each the sum of k independent experimental values sampled from the same normal distribution. At edges, each of LS and RS is the sum of $k_1$ independent experimental values drawn from the normal distribution that represents one of the coloring processes and $k_2$ independent experimental values from the normal distribution that describes the other coloring process. The sum of $k_1$ and $k_2$ is k, but $k_1$ and $k_2$ will in general vary from point to point on the image line.

The assumption of normality of $e_k$ at edges will hold well if the variances of $k_1$ and $k_2$ are low. This means that in the neighborhood of any edge point on the image line the number of pixels colored by either process remains almost constant. For example, this is trivially true for the constant distribution of cell widths, with $k \leq b$, b being the width of a cell. In this extreme case, $k_1 = k$ and $k_2 = 0$ or vice versa. However, if $k_1$ and $k_2$ have a high variance, then the normality assumption will not hold very well.

Thus, an important factor for the validity of the assumption is the variance of cell widths. Ideally, this variance should be small; however another property that would tend to make the assumption hold well is that the image model be more likely to contain cells whose widths are close to k. This will keep the probability that the neighborhoods $C_\ell$ and $C_r$ extend

over more than one cell quite low.

Given the normality assumption, the following two step process can be used to compute an optimal k and t for a minimum error edge detector.

1) For a range of k, find the minimum error threshold for discriminating between edges and interior points. Since both $e_k$ at edges and $e_k$ at interior points are modeled by normal distributions with known parameters and priors, this is straightforward. Let er(k) be the probability of error for the minimum error threshold for $e_k$ and let t(k) be the threshold.

2) Choose k such that er(k) $\leq$ er(k'), for all k' considered. Then (k,t(k)) define the minimum error edge detector.

Figure 2 shows plots of er(k) as a function of k for the three cell width models presented in Section 2. Notice that the value of k which minimizes total errors is the mean cell width for all three models. The reason that the curves tend to level off at high k, rather than rise to a high error, is that as k becomes very large, the prior probability of interior points, $p_i$, approaches zero. For very high values of k, the near zero value of $p_i$ causes the programs which compute minimum error thresholds to become unstable. Therefore, we arbitrarily stopped computing er(k) for $k > 20$. Figure 3a-e shows an example of the effect of k on the performance of $e_k$. Figure 3a contains a checkerboard texture with $b = 16$, $p = .5$, $m_1 = 30$, $m_2 = 20$, and $v_1 = v_2 = 10$. Figure 3b shows the true edges, while Figures 3c-e show the results of applying $e_k$, $k = 8$, 16 and 24, thresholding at the minimum error threshold for the appropriate k, and then performing non-maxima suppression across 8 pixels. Note that the results for the optimal value of k (16) are significantly better than choosing k too small (8) or too large (24).

## 5. Discussion

This paper has discussed the problem of detecting edges in cellular textures. A general edge detection procedure was proposed. This procedure involved applying an edge sensitive operator to the texture, and then thresholding the results of the edge operator and finally computing "peaks" from the above threshold points. This paper concentrated on the thresholding process and developed a minimum error thresholding procedure based on an analysis of the edge operator $e_k$. The thresholding procedure assumed that $e_k$ was normally distributed at edges and at interior points.

The peak selection step was not considered in this paper. It is discussed in [20], which also includes examples of choosing optimal edge detectors for real textures, and a comparative classification study using optimal and suboptimal edge detectors.

## References


1. N. Nahi and S. Lopez-Mora, "Estimation detection of object boundaries in noisy images," *IEEET-Automatic Control, 23,* 1978, 834-846.

2. J. Modestino and R. Fries, "Edge detection in noisy images using recursive digital filtering," *Computer Graphics and Image Processing, 6,* 1977, 409-433.

3. K. Shanmugan, F. Dickey and R. Dubes, "An optimal frequency domain filter for edge detection in digital pictures," *IEEET-Pattern Analysis and Machine Intelligence, 1,* 1979, 37-49.

4. D. Cooper and H. Elliot, "A maximum likelihood framework for boundary estimation in noisy images," Proc. IEEE Computer Society Conf. on Pattern Recognition and Image Processing, Chicago, IL, May 31-June 2, 1978, 25-31.

5. A. Rosenfeld and A. Kak, *Digital Picture Processing,* Academic Press, New York, 1976.

6. J. Weszka, C. Dyer and A. Rosenfeld, "A comparative study of texture features for terrain classification," *IEEET-Systems, Man and Cybernetics, 6,* 1976, 269-285.

7. D. Marr, "Early Processing of Visual Information," *Phil. Trans. Royal Society, B, 275,* 1976, 483-524.

8. L. Davis, S. Johns and J. K. Aggarwal, "Texture analysis using generalized cooccurrence matrices," *IEEET-Pattern Analysis and Machine Intelligence, 1,* 1979, 251-258.

9. L. Davis, M. Clearman and J. K. Aggarwal, "A comparative texture classification study based on generalized cooccurrence matrices," to appear in IEEE Conf. on Decision and Control, Miami, FL., Dec. 12-14, 1979.

10. N. Ahuja, "Mosaic models for image synthesis and analysis," Ph.D. dissertation, University of Maryland, Computer Science Dept., 1979.

11. B. Horn, "Understanding image intensities," *Artificial Intelligence, 8,* 1977, 208-231.

12. B. McCormick and S. Jayaramamurthy, "Time series models for texture synthesis," *J. Computer and Information Sciences, 3,* 1974, 329-343.

13. J. Tou, D. Kao and Y. Chang, "Pictorial texture analysis and synthesis," Proc. Third Int. Joint Conf. on Pattern Recognition, Coronado CA., Nov. 8-11, 1976, 590.

14. E. Wong, "Two-dimensional random fields and representations of images," *SIAM J. Applied Math., 16,* 1968, 756-770.

15. W. Pratt and O. Faugeras, "Development and evaluation of stochastic-based visual texture fields," Proc. 4th Int. Joint Conf. on Pattern Recognition, Nov. 1978, 545-548.

16. M. Hassner and J. Sklansky, "Markov random fields of digitized image texture," Proc. 4th Int. Joint Conf. on Pattern Recognition, Nov. 1978, 538-540.

17. K. Abend, I. Harley and L. Kanal, "Classification of binary random patterns," *IEEET-Information Theory, 11,* 1965, 538-544.

18. M. Duff, "CLIP-4: A large scale integrated circuit array parallel processor," Proc. 3rd Int. Joint Conf. on Pattern Recognition, 1976, 728-732.

19. B. Kruse, "A parallel picture processing machine," *IEEET-Computers, 22,* 1973, 1075-1087.

20. L. Davis and A. Mitiche, "Optimal texture edge detection procedures," in preparation.

21. A. Drake, *Fundamentals of Applied Probability Theory,* McGraw-Hill, New York, 1967.

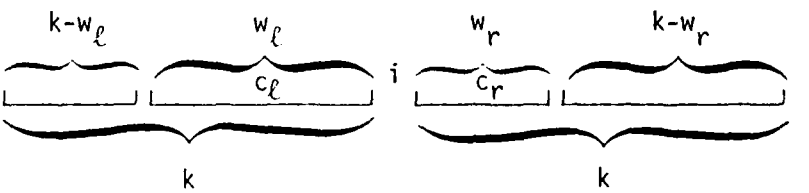


Figure 1. Neighborhood of an edge point, i.

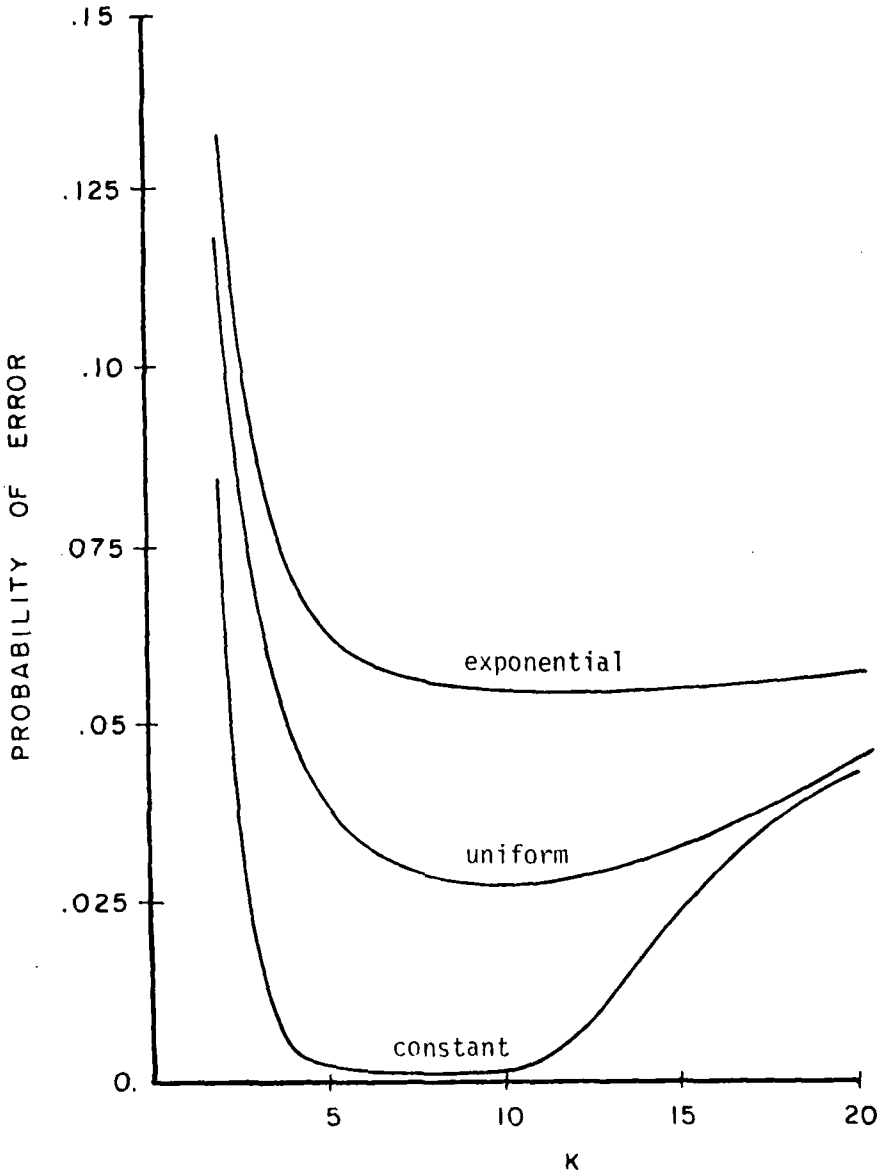


Figure 2. Plots of er(k) as a function of k for the three cell width models. All parameters are the same for all three models: $m_1 = 10$, $m_2 = 5$, $v_1 = v_2 = 2$, $p = .5$ and $w_0 = 10$.

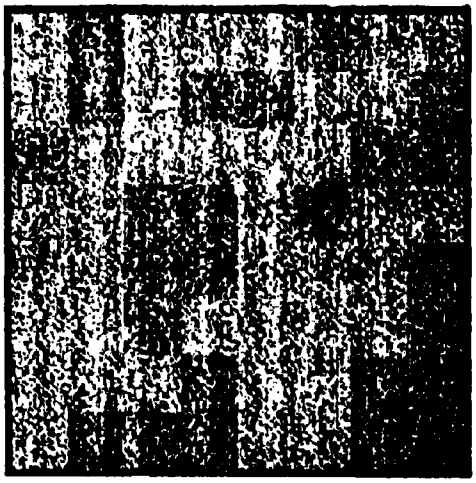

a) original texture

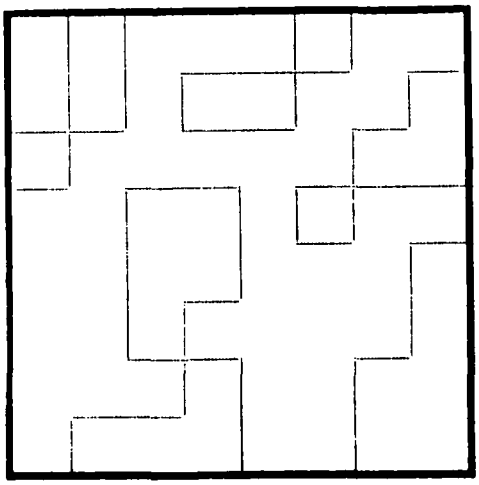

b) true edges

Figure 3. Application of $e_k$ to a checkerboard texture.

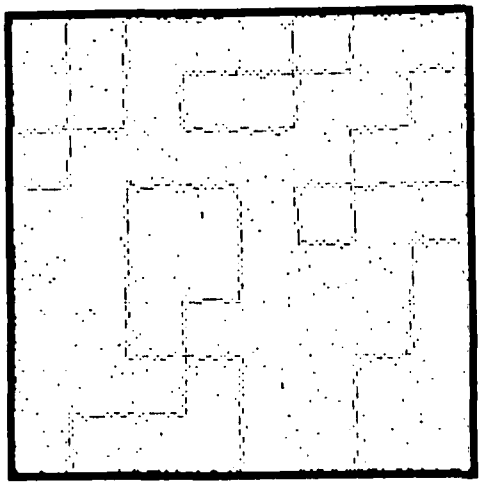

c) k = 8

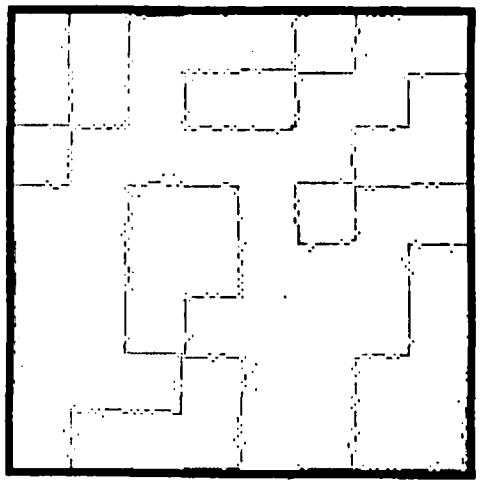

d) k = 16

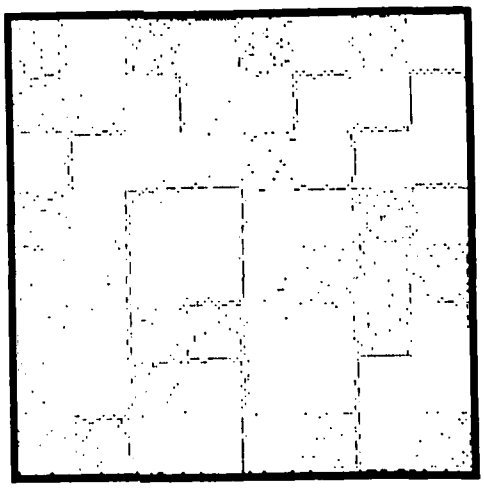

e) k = 24

Figure 3. continued.

D

FI

6